Available online at www.sciencedirect.com
ScienceDirect
Journal of the European Ceramic Society 29 (2009) 1147–1155
www.elsevier.com/locate/jeurceramsoc

Micromoulding of PZT film structures using electrohydrodynamic atomization mould filling

D. Wang *, S.A. Rocks, R.A. Dorey

Microsystems & Nanotechnology Centre, Cranfield University, Bedfordshire MK43 0AL, UK

Received 17 June 2008; received in revised form 4 August 2008; accepted 12 August 2008
Available online 26 September 2008

Abstract

In this work, electrohydrodynamic atomization combined with a photolithography polymeric micromoulding technique was used to form PZT ceramic structures. PZT thick film structures consisting of squares and rectangles of various sizes and separations were produced and used to evaluate the process. An expansion effect of approximately 10 μm on the ceramic structure width relative to the 200 μm wide mould design was observed. The minimum continuous gap between features achieved using this process was 13.5 μm, and the smallest regular PZT square structure obtainable was 106 μm in width. A sloping side wall of the PZT structures caused by the shielding of the photoresist mould was also observed in the process. The resulting PZT structures had a homogenous microstructure and exhibited a relative permittivity of 250, $d_{33,f}$ of 67 pCN^{-1} and remnant polarisation of 8.8 $\mu C/cm^2$.

Keywords: PZT; Films; Suspensions; Micromoulding; Ferroelectric properties

1. Introduction

10–100 μm thick piezoelectric film is of great interest for micro-electromechanical system (MEMS) applications such as sensors, transformers, transducers and actuators.[1–4] Within these applications, lead zirconate titanate (PZT) is an important piezoelectric material because of its high piezoelectric constant, relative permittivity and electromechanical coupling coefficient.[5] Fabrication of such thickness PZT films using current fabrication methods is limited by low deposition rate (physical vapour deposition),[6] high processing temperature (screen printing),[7] and stress generation (sol-gel coating).[8] Conversely, the use of conventional bulk ceramic processing with subsequent machining and bonding is wasteful of material and time consuming.[9]

The formation of PZT thick film structures is another critical issue for the integration of PZT onto MEMS. Two typical routes are commonly used, one of which is screen printing, and the other is chemical wet etching of previously deposited continuous films. However, a high sintering temperature (850–1200 °C) is needed in screen printing, which can damage the substrate and electrodes.[10] In addition the resolution is limited between 25 and 100 μm for screen printing by the mesh size and ability to accurately deposit multiple layers on top of each other.[11] The wet etching of ceramic films can lead to sloping slide walls and limited resolution due to the isotropic etching process.[12] Moreover, the chemical etching solution is hazardous as it contains hydrofluoric acid. Recently, a new fabrication route using a micromoulding process in conjunction with a composite sol–gel spin coating technique was developed to produce ceramic structures.[13] The advantage of this process is: 1) low sintering temperature due to the use of the composite sol–gel material and 2) the possibility of producing high resolution structures through the use of micromoulds.

The deposition methods commonly utilized in micromoulding processes are mainly contact coating techniques such as spin coating or screen printing, which limit the edge resolution of the structures produced because of flow build up at the walls of the micromould during the removal of excess ceramic suspension. This leads to a characteristic "U" shaped profile of the feature and a risk of edge fracture. One potential method to overcome this limit is the use of a spray deposition technique for coating, which provides a purely vertical deposition of

* Corresponding author. Tel.: +44 1234 750111x2723; fax: +44 1234 751346.
E-mail address: d.wang@cranfield.ac.uk (D. Wang).

0955-2219/$ – see front matter © 2008 Elsevier Ltd. All rights reserved.
doi:10.1016/j.jeurceramsoc.2008.08.018

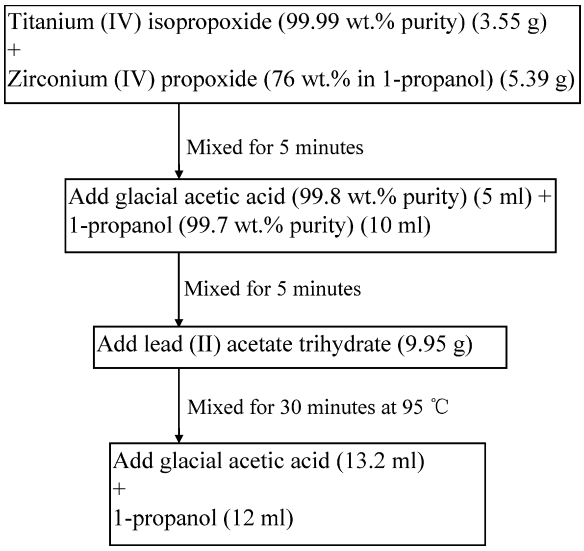

Fig. 1. Flow chart illustrating the propanol-based PZT sol preparation route.

PZT ensuring uniform coverage and thickness. Ink-jet printing (IJP) is commonly used in the direct forming of ceramic structures.[14] However, the drawback of this method is that the printed droplet size depends on the nozzle size. To achieve small droplets requires small nozzles which lead to needle blockage when using highly viscous suspensions containing large particles. Electrohydrodynamic atomization (EHDA) makes use of

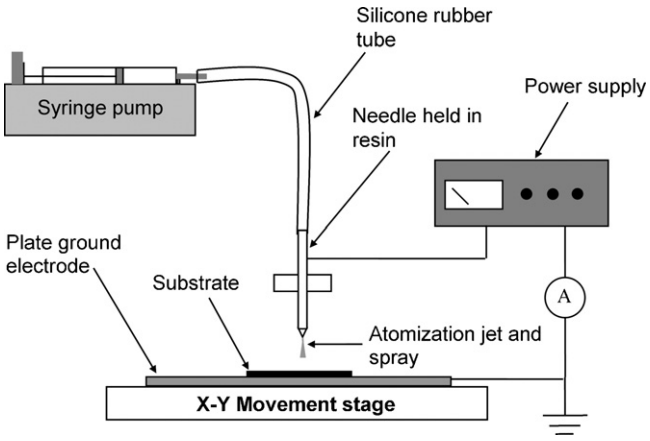

Fig. 2. Schematic representation of EHDA deposition equipment set-up.

electrical and mechanical forces to form a liquid jet and disintegrate it into droplets.[15] This makes it possible to produce fine droplets using a coarse nozzle with a dependence on electrohydrodynamic force rather than the nozzle size. The EHDA process was widely used in coating[16] and generation of fine powders and droplets from liquids.[17] The use of suspensions in EHDA has shown great potential in recent years.[18–20] In this work, the EHDA technique is employed in the micromoulding process to form ceramic structures by depositing dense and crack-free PZT films from a PZT composite sol–gel slurry into polymeric moulds.

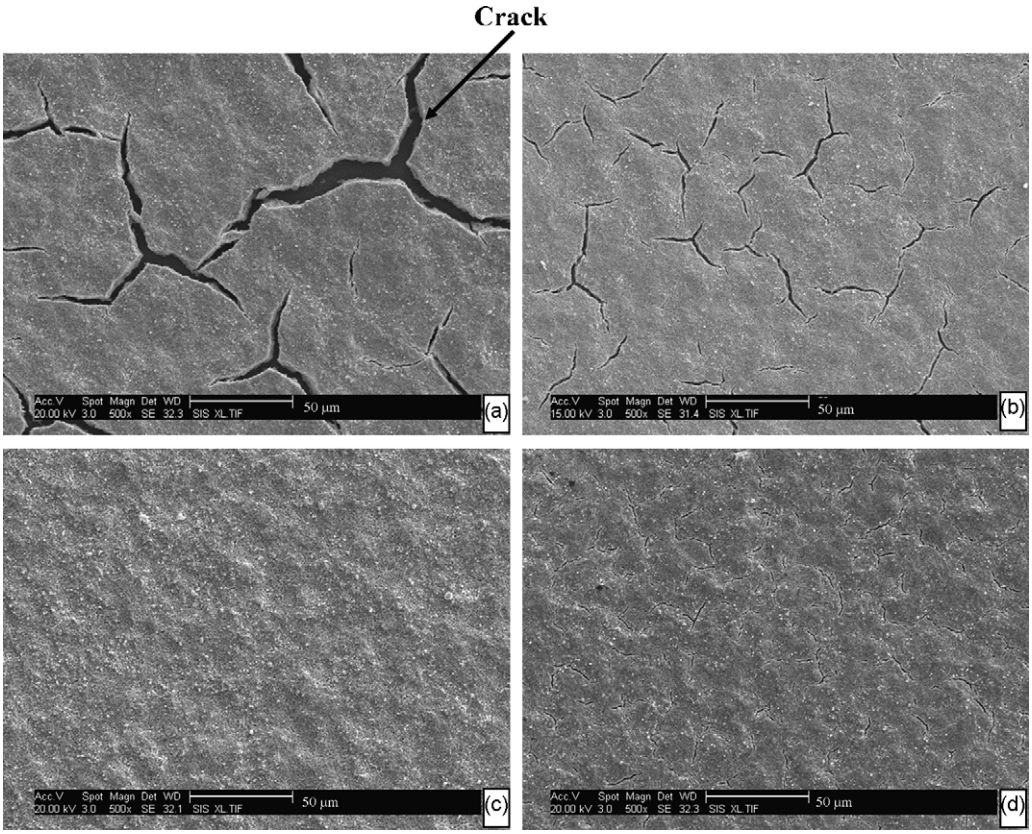

Fig. 3. Scanning electron microscope micrographs showing the surface of 20 layer PZT films produced using different intermediate solvent removed processes: (a) dry at room temperature for 5 min, (b) dry at 100 °C for 2 min, (c) dry at 100 °C for 5 min and (d) vacuum at 1.3 kPa for 5 min at room temperature.

2. Experimental details

2.1. Mask design

Three types of feature were designed on a 4 in. Chromium/glass photomask. One feature type was a series of squares with widths varying from 1 μm to 2000 μm with the gap between the squares fixed at 200 μm; another feature type had gaps varying in width from 1 μm to 300 μm between a series of 200 μm wide squares. The third feature was a series of 200 × 4425 μm rectangles with gaps varying in width from 1 μm to 300 μm. Using these test features, capabilities in terms of feature size and resolution of the technique were explored along with the ability to form elongated channels.

2.2. Polymeric micromould formation

Prior to deposition of the photoresist, the Si wafer was coated with a blanket layer of Ti/Pt (8/100 nm) using RF magnetron sputtering (Nordiko Ltd., Hampshire, UK) and cleaned using acetone/propan-1-ol on a spinner and then dried at 100 °C for 3 min. Three layers of AZ9260 positive photoresist (MicroChemicals GmbH, Ulm, German) were spun onto a 4 in. silicon wafer to achieve a polymer film approximately 38 μm thick which is designed to meet the thickness of the PZT film (∼30 μm) to be obtained for the ultrasonic transducer requirement.[21] The first layer of photoresist was spun down at 2400 rpm for 60 s, and then baked on a hot plate at 100 °C for 160 s. The second and third layers were spun down at 2100 rpm for 60 s, and then baked at 110 °C for 160 s. In order to remove the bead formed at the edge of the wafer during spinning, the edge of the wafer was carefully washed with acetone using a cotton bud, spun at 1500 rpm for 60 s and dried on a hot plate at 100 °C for 30 s. The spin coated photoresist was then exposed to UV light on a MA56 mask aligner (SUSS MicroTec. Lithography GmbH, Garching, Germany) at a beam intensity of 6.2 mW cm^{-2} for 403 s. The polymer micromould structures were developed in the solution of diluted AZ400K (1:4 in water) for approximately 8 min to obtain the micromould features. After being cleaned with distilled water the micromoulds were dried at 100 °C for 120 s before the EHDA deposition of PZT films.

2.3. EHDA deposition of PZT

The PZT composite sol-gel slurry was prepared from 10 g of PZT powder with a mean particle size of approximately 0.6 μm and chemical composition of Pb 1: Zr 0.481: Ti 0.472:

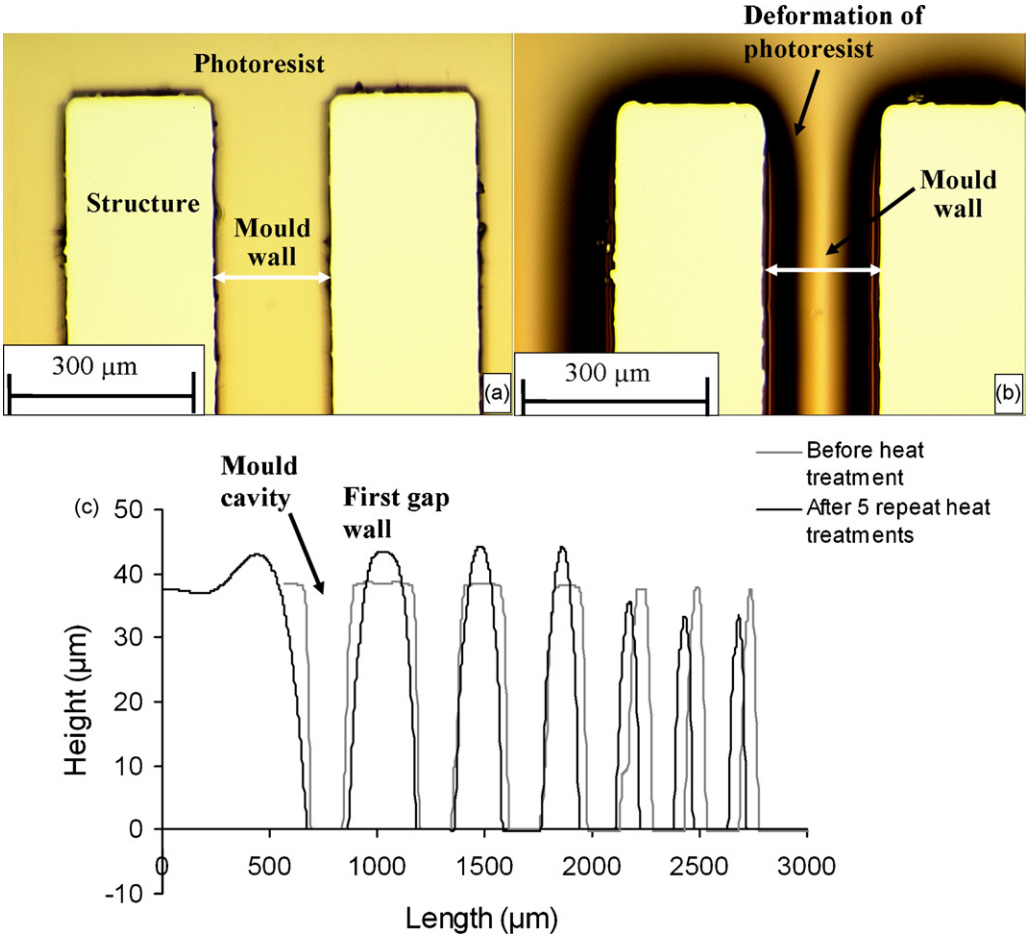

Fig. 4. Optical micrographs and surface profile analysis showing the influence of the repeated heat treatment process at 100 °C for 5 min on the photoresist micromould: (a) before heat treatment, (b) after 5 repeat heat treatment process and (c) the surface profile of (a) and (b).

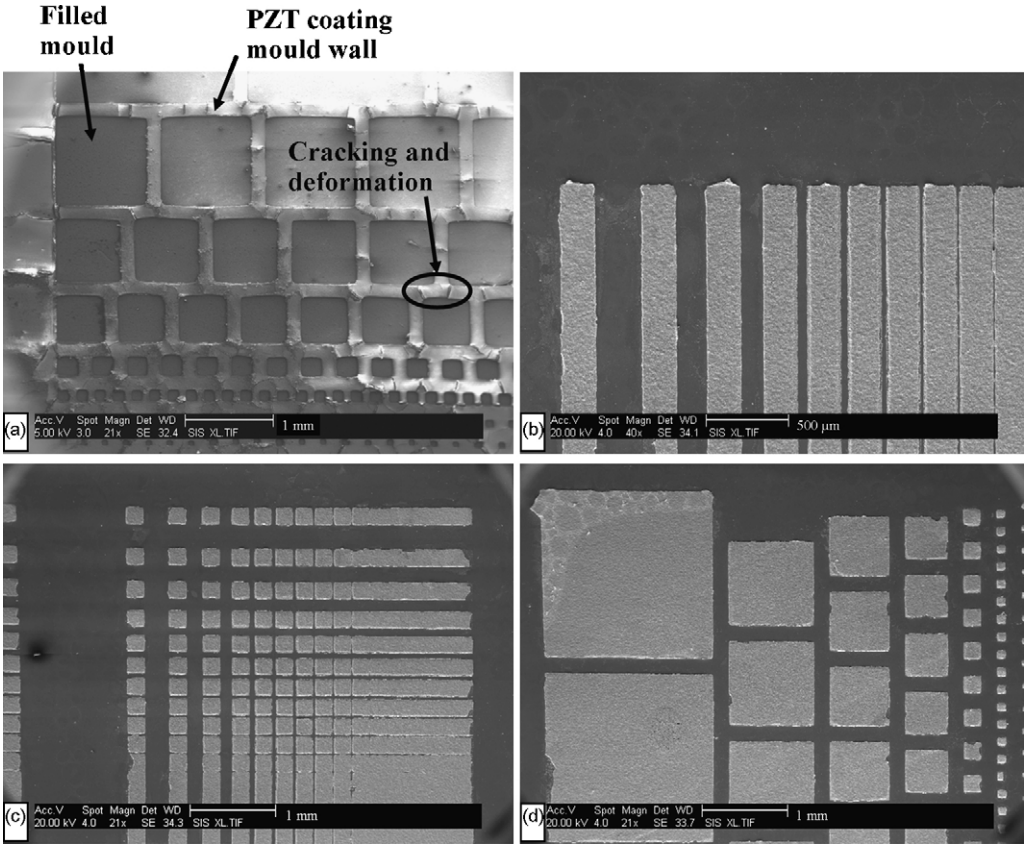

Fig. 5. Scanning electron microscope micrographs showing the PZT film structure after 60 EHDA deposition layers at the drying process of 100 °C for 5 min at every two layers intermediate: (a) on the polymeric micromould before sintering, (b) sintered and patterned 200 μm wide rectangles with gaps of varying sizes, (c) sintered and patterned 200 μm wide squares with gap of varying lengths and (d) sintered and patterned squares of different sizes.

Nb 0.015: Sb 0.015:Mn:0.015: (PZ 26, Ferroperm, Denmark), 14.2 ml of PZT sol (0.42 M), 0.2 g of dispersant KR 55 (KenReact Lica 38, KenRich) which was used to stabilize the slurry and 0.069/0.428 g of Cu_2O/PbO sintering aid which helps to increase the density and piezoelectric properties of the sintered PZT film. All these components were mixed in a nitrogen environment and then ball-milled on a roller for 24 h. The PZT sol was prepared from the precursors lead (II) acetate trihydrate, titanium (IV) isopropoxide and zirconium (IV) propoxide. The preparation route is illustrated in Fig. 1. The final chemical stoichiometric ratio of the metal ions in the PZT sol were Pb 1.10: Zr 0.48: Ti 0.52.

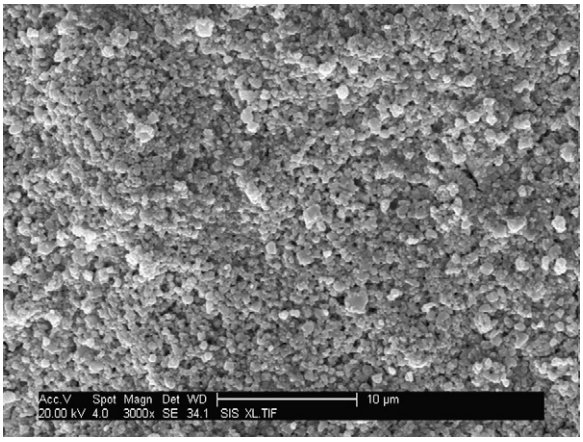

Fig. 6. Scanning electron microscope micrograph showing the surface microstructure of the patterned PZT film structure after 60 EHDA deposition layers.

The EHDA deposition device is comprised of an electrohydrodynamic needle coupled with a computer controlled *X-Y* movement stage (Fig. 2). A needle was connected to a high voltage power supply and its inlet was connected to a syringe pump using a silicone rubber tube through which PZT slurry was pumped. The inner and outer diameter of the needle is 0.85 and 1.3 mm which is a standard commercially available size. Needles smaller than this size are easily blocked by the flowing slurry during EHDA process. The high voltage power supply (Glassman High Voltage Inc., NJ, USA) was used to apply an electric field between the needle and the ground electrode, and a syringe pump (KD Scientific Inc., MA, USA) was employed to provide the hydrodynamic force to push the PZT slurry up to the outlet of the needle. A thin aluminium plate, serving as the ground electrode, was placed directly on the *X-Y* movement stage and connected to earth potential.

The micromould wafer was placed on the aluminium plate ground electrode 1 mm below the needle exit for EHDA deposition. In order to obtain a stable jet, the flow rate and the applied voltage were kept constant at $2.2 \times 10^{-10}\,m^3\,s^{-1}$ and 5.5 kV during deposition. The PZT film was built up by alter-

Table 1
The comparison between design and PZT structure on the squares with different width

Design	PZT structure (μm)	Expansion of PZT structure in width according to the design (μm)	Standard deviation	Expansion of PZT structure in width according to the design %
2000	2019.1	19.1	8.7	0.95
1000	1010.2	10.2	5.5	1.02
700	712.3	12.3	2.2	1.77
500	514.2	14.2	4.5	2.84
200	208.7	8.7	4.1	4.35
100	106.3	6.3	4.1	6.3
70	69.3 (NR)*	−0.7	4.4	NR
50	N/A	N/A	N/A	N/A

* NR: structure not regular.

nately depositing in the *X* and *Y* directions on the mould for 60 layers. During the deposition a scan speed of 39 mm s^{-1} and a distance of 4 mm between two neighbouring parallel paths of deposition were set to ensure a degree of overlap between deposited materials. After every two intermediate layer depositions (one *X* direction scan and one *Y* direction scan) the PZT film was subjected to a solvent removing process. During evaporation of the solvent in the PZT film, shrinkage occurs which can generate internal stress, resulting in cracking of the film. In order to prevent this and obtain dense and crack-free PZT films intermediate drying is used after the deposition of individual layers.[22] Ideally this is conducted at a sufficiently high temperature to cause complete conversion of the sol-gel material. Due to the presence of the polymeric mould material, high temperatures are not appropriate. Four conditions were examined in this process to assess the effect on the film microstructure: (1) drying at room temperature for 5 min, (2) drying at 100 °C for 2 min, (3) drying at 100 °C for 5 min and (4) vacuum drying at 1.3 kPa at room temperature for 5 min.

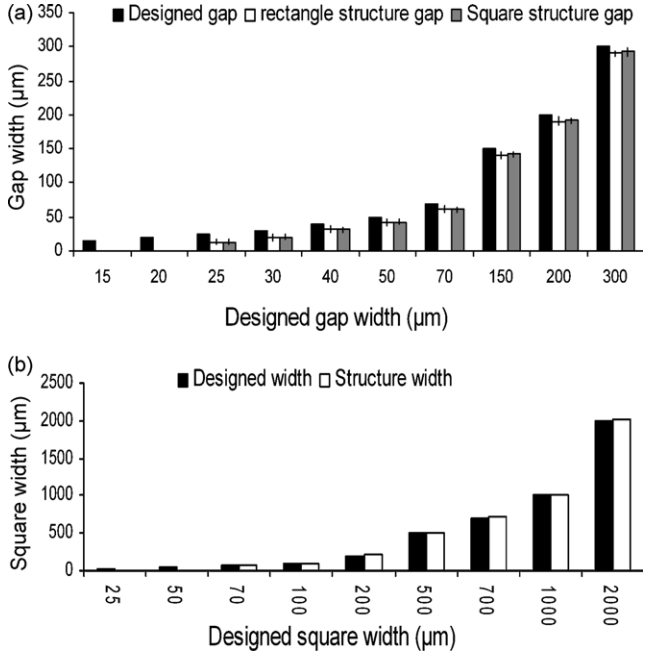

Fig. 7. The comparison of design and deposited PZT film structures: (a) 200 μm width rectangles and squares with gaps of varying size and (b) squares of different size.

2.4. PZT structure evaluation

In order to remove the polymeric mould and pyrolyze the PZT film after EHDA deposition, the structure was sintered at 720 °C for 20 min in a muffle furnace. The final PZT film structure was dipped in acetone for 5 min and then cleaned in an ultrasonic bath to remove residual photoresist. Chromium/gold top electrodes with a thickness of 15/100 nm and a diameter of 770 μm were deposited on the PZT film structure surface by vacuum evaporation (Edwards Evaporator E480) after sintering to allow electrical characterisation.

3. Results and discussion

3.1. Formation of crack-free PZT films

Fig. 3 shows the sintered surface finish of 20 layer thick films produced using the drying condition at: (a) room temperature, (b) 100 °C for 2 min, (c) 100 °C for 5 min and (d) under vacuum at room temperature. Before sintering no distinct cracks were evident on the films subjected to the heating and vacuum drying processes. After sintering the PZT film produced using the room temperature intermediate drying process showed large cracks (Fig. 3a), which resulted from the shrinkage induced by the removal of large quantities of residual solvent in the film leading up to the final sintering stage. When a drying temperature of 100 °C for 2 min was applied to the film the cracking was reduced (Fig. 3b) but not eliminated. A 5 min drying time at 100 °C was shown to be adequate to remove the solvent sufficiently to obtain crack-free films (Fig. 3c). AZ9260 photoresist is intolerant to high temperatures, and temperatures higher than 110 °C resulted in its rapid deformation and degradation presenting the use of more thermally extreme drying conditions. Therefore, the intermediate heat treatment process at 100 °C for 5 min was used as drying condition to remove the solvent and obtain crack-free PZT film using this technique. The film was also subjected to a vacuum treatment at 1.3 kPa for 5 min to force the solvent volatilisation without the application of heat. Small cracks were still evident after this treatment and sintering

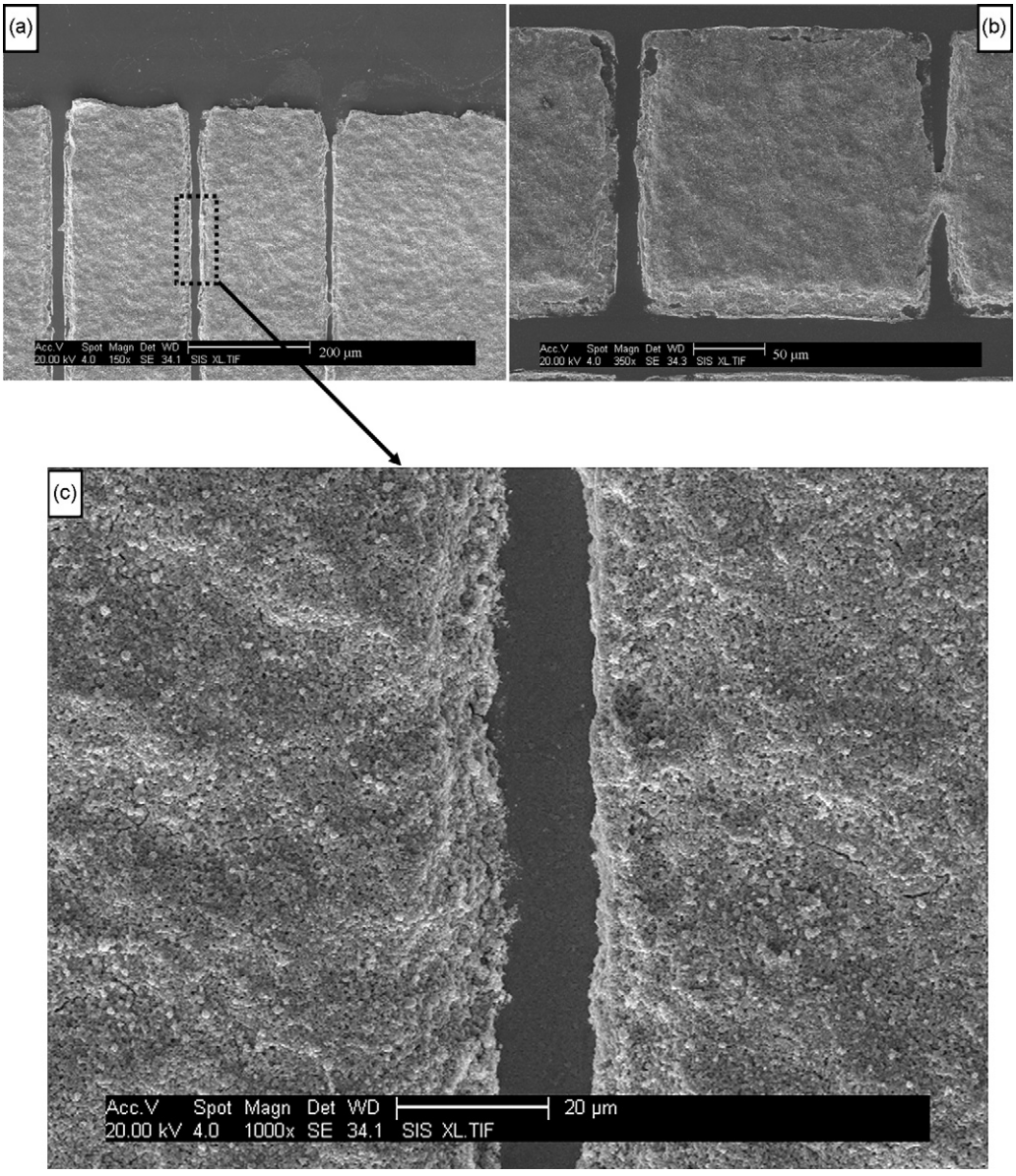

Fig. 8. Scanning electron microscope micrographs showing the microstructure of the smallest gap patterned after 60 EHDA deposition layers: (a) between 200 μm wide rectangle PZT structures, (b) between 200 μm wide square PZT structures and (c) appearance at a high magnification.

(Fig. 3d), showing that insufficient evaporation of the solvent during this process had occurred.

3.2. Formation of PZT structures

3.2.1. Effect of heat treatment on polymeric mould

Due to the repeated thermal cycling of the mould material during drying it is important to understand how it changes in shape during this process. The comparisons of a 200 μm wide rectangle photoresist micromould separated by different gaps, before and after 5 repeat 100 °C/5 min heat treatments are shown in Fig. 4. Before heating, the photoresist mould presented flat even thickness (~38 μm) surfaces and vertical sidewalls (Fig. 4a). However, after 5 repeat heat treatment processes the deformation of the photoresist was evident (black colour) and the shape of the moulds became irregular (Fig. 4b). This was caused by the evaporation of the residual solvent and water and the degradation of the photoactive compound during the heating process.[23,24] While the majority of the solvent and water is removed during the soft baking process before expose, some remains and longer soft baking times have been shown to lead the degradation of the photoactive compound and deteriorate the function of the resist.[24] The surface profiles of the photoresist mould before and after the heat treatments is shown in Fig. 4c and highlight the deformation that has occurred during heat cycling. It was calculated that the volume shrinkage of the photoresist on the first mould wall was 15.5 vol%, and the average width expansion of the 200 μm wide photoresist mould cavity structure was 5 μm after 5 repeat heat treatment processes.

3.3. Feature of PZT structures

Fig. 5a shows the polymeric micromould coated with 60 EHDA deposited layers of PZT before sintering. The PZT film on the Si substrate presents as a flat surface, while the PZT on the photoresist material exhibits deformation and cracking after several repeat heat treatment processes. The sintered patterned PZT film structures of rectangles and squares of different gaps and sizes obtained after 60 EHDA deposition layers and photoresist removal are shown in Fig. 5b, c and d. Fig. 6 shows the surface of the patterned PZT film structure after sintering presenting a well-packed and crack-free film. The comparison of the design and deposited PZT film structure dimensions for the three types of structure is illustrated in Fig. 7 and Table 1. After sintering the patterned PZT rectangle and square structure was 210 μm wide relative to a 200 μm design, which resulted in a 10 μm reduction in the gap between neighbouring structures (Fig. 7a). The expansion behaviour of the deposited PZT structure is due to the enlargement of the polymeric mould cavity during the drying process. It was observed that the polymeric mould cavity exhibited a 15 μm increase in width according to the nominal 200 μm wide rectangle and square structure design. Irregular features at the corner and delamination behaviour at the edge of the PZT structure were observed (Fig. 5b, c and d) which was caused by the deformation of the photoresist during the drying process (Fig. 4).

The minimum resolvable gap separating the PZT rectangles and squares produced was 13.5 μm (Fig. 8) which corresponded to the smallest (12.5 μm) width of photoresist micromould wall that was obtainable and a 25 μm wide design. The smallest regular PZT square structure produced was 106 μm in width (Fig. 9a). Features smaller than this size (69 μm) were irregular (Fig. 9b) in shape. The surface profile of the 106 μm and 69 μm wide PZT structures are shown in Fig. 9c and d. The surface profile of the 69 μm wide PZT square presents a much shallower wall slope (22°) (Fig. 9d) than that of the 106 μm wide structure (34°) (Fig. 9c). The sloping side wall extended for approximately 20 μm (Fig. 9c and d) which resulted in nearly no top surface region on the 69 μm wide PZT square structure explaining why only features larger than 69 μm could be obtained.

Fig. 10a shows a typical cross section of the edge of a PZT square structure, which presents a dense and well packed PZT film. A sloping side wall was also observed on this structure. Previously such features were attributed to edge fractures during mould removal. However, after examination of a similar cross section with the mould still in place it can be seen that this sloping side wall is caused by the deformation of the polymer micromould during the heat treatment process and the formation of a stack of PZT on the mould edge during EHDA deposition which shielded the edge of the underlying PZT structure (Fig. 10b). A shielding effect distance of ~20 μm was observed on this cross section which corresponds to the extension of the sloping side wall observed during the surface profile analysis of the PZT square structures (Fig. 9c and d).

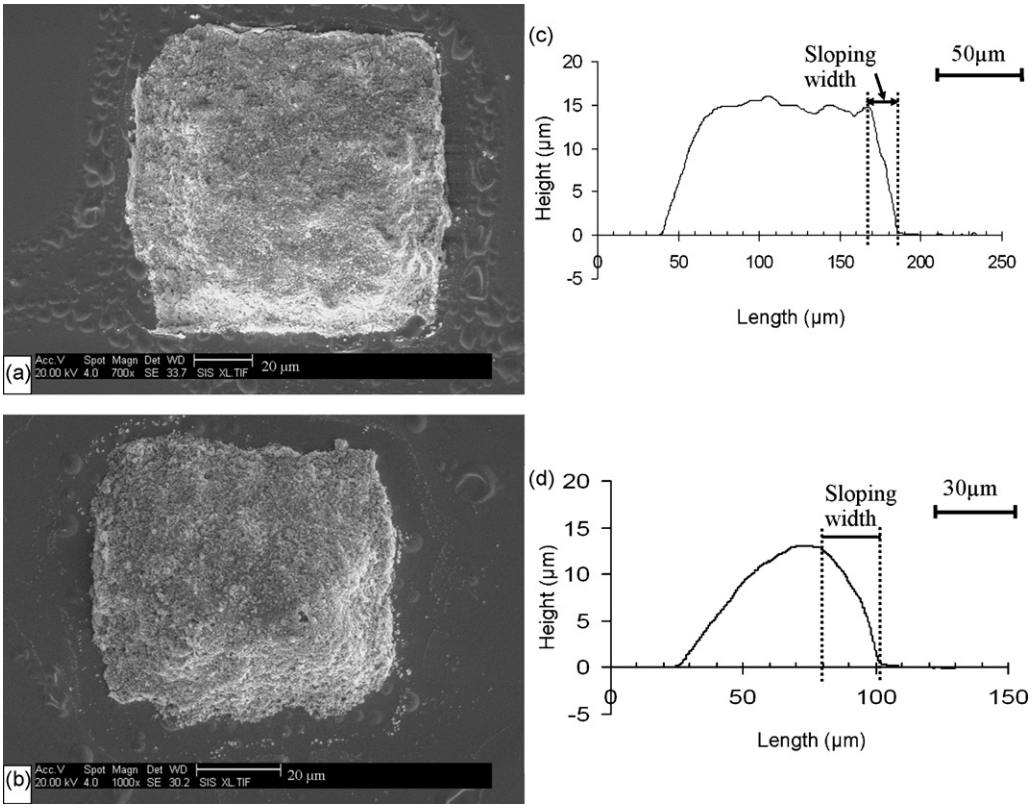

Fig. 9. Scanning electron microscope micrographs and surface profile analysis showing the microstructure of the patterned PZT square: (a) a 105 μm in width and its surface profile (b); and (c) a 67 μm in width and its surface profile (d).

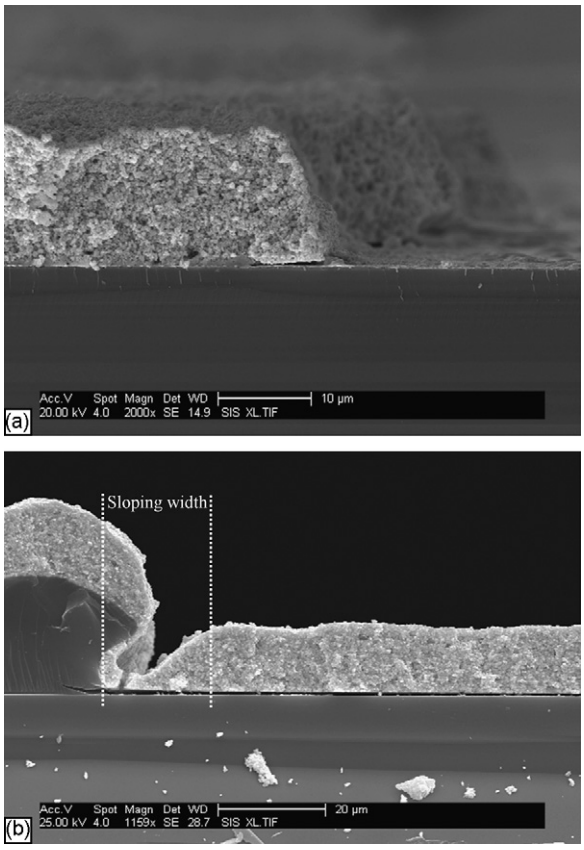

Fig. 10. Scanning electron microscope micrographs showing the cross-section of a) the patterned PZT film structure on the polymer micromould after 60 EHDA deposition layers and b) a typical polymer micromould of 42 μm in width.

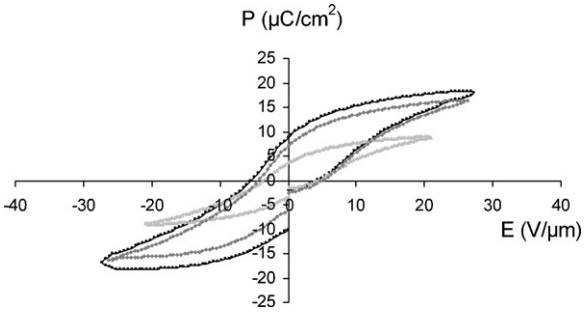

Fig. 11. The PZT film structure hysteresis loop.

3.4. Electrical characterisation

The relative permittivity (ε_r) of the PZT structures was calculated to be 250 (±8) with a dielectric loss of 0.02. The ferroelectric hysteresis loops of a PZT film structure at different applied electric fields are shown in Fig. 11. The film becomes saturated at the maximum electric field intensity of 27 V μm^{-1}. The film exhibits a lower remnant polarisation (P_r) than the corresponding bulk material at a comparable field. The low value of the relative permittivity and remnant polarisation is mainly due to the existence of pores in the films and presence of the rigid substrate constraining the film. The highest film piezoelectric constant ($d_{33,f}$) obtained was 67 pCN^{-1} when poled at 11 V μm^{-1} at 200 °C for 5 min, which is comparable to the composite films produced using the spin-coating technique and screen printed PZT.[25,26] The ε_r and $d_{33,f}$ of the PZT structures are also comparable to the results obtained from continuous films prepared using the EHDA technique. Work on continuous films has shown that the ferroelectric, piezoelectric and dielectric properties can be improved by increasing the density of the films using a higher temperature drying process and PZT sol infiltration process.[27] Future work will examine this possibility.

4. Conclusions

The use of electrohydrodynamic atomization deposition combined with a photolithography polymer micromoulding technique to form PZT ceramic structures was demonstrated. Three types of PZT film structure were designed and produced. Minimum regular PZT square sizes and separations produced were 106 μm and 13.5 μm, respectively. It was observed that the photoresist mould cavity increased in size by 15 μm for a 200 μm design and the PZT structure reduced in width by 5 μm compared with the photoresist mould cavity. Therefore, a 10 μm allowance in advanced design is needed to obtain the desired structure using this process. The piezoelectric coefficient ($d_{33,f}$) of 67 pCN^{-1} and relative permittivity (ε_r) of 250 were obtained for this PZT film structure, which can be improved further by increasing the density and reducing the roughness of the films. This process provides a new way for forming PZT microstructures, with the advantage of high resolution, fast speed and no reliance on harsh etching which are suitable for the requirement of MEMS device fabrication.

Acknowledgements

Dr. Christopher Shaw and Mr. Andrew Stallard are thanked for their generous help with this work. This work is funded by EPSRC (GR/84156/01), the European commission as part of the MIND (Multifunctional & Integrated Piezoelectric Device) project and the Piezo Institute. Dr Robert Dorey is a Royal Academy of Engineering/EPSRC research fellow.

References

1. Gebhardt, S., Seffner, L., Schlenkrich, F. and Schonecker, A., PZT thick films for sensor and actuator applications. *J. Eur. Ceram. Soc.*, 2007, **27**, 4177–4180.
2. Kim, H., In, C., Yoon, G. and Kim, J., Design and fabrication of a micro PZT cantilever array actuator for applications in fluidic systems. *J. Mech. Sci. Technol.*, 2005, **19**, 1544–1553.
3. Kozielski, L., Lisinska-Czekaj, A. and Czekaj, D., Graded PZT ceramics for piezoelectric transformers. *Prog. Solid State Ch.*, 2007, **35**, 521–530.
4. Zhang, Q. Q., Djuth, F. T., Zhou, Q. F., Hu, C. H., Cha, J. H. and Shung, K. K., High frequency broadband PZT thick film ultrasonic transducers for medical imaging applications. *Ultrasonics*, 2006, **44**, E711–E715.
5. Haertling, G. H., Ferroelectric ceramics: history and technology. *J. Am. Ceram. Soc.*, 1999, **82**, 797–818.
6. Zhou, Q. F., Chan, H. L. W. and Choy, C. L., Conducting lanthanum nickel oxide as electrodes for lead zirconate titanate films. *Thin Solid Films*, 2000, **375**, 95–99.
7. Thiele, E. S., Damjanovic, D. and Setter, N., Processing and properties of screen-printed lead zirconate titanate piezoelectric thick films on electroded silicon. *J. Am. Ceram. Soc.*, 2001, **84**, 2863–2868.

8. Dauchy, F. and Dorey, R. A., Patterned high frequency thick film MEMS transducer. *Integr. Ferroelectr.*, 2007, **90**, 42–52.
9. Le Dren, S., Simon, L., Gonnard, P., Troccaz, M. and Nicolas, A., Investigation of factors affecting the preparation of PZT thick films. *Mater. Res. Bull.*, 2000, **35**, 2037–2045.
10. Mass, R., Koch, M., White, N. M. and Evans, A. G. R., Thick-film printing of PZT onto silicon. *Mater. Lett.*, 1997, **31**, 109–112.
11. Torah, R. N., Beeby, S. P., Tudor, M. J. and White, N. M., Thick-film piezoceramics and devices. *J. Electroceram.*, 2007, **19**, 95–110.
12. Dauchy, F. and Dorey, R. A., Patterned crack-free PZT films for microelectromechanical system applications. *Int. J. Adv. Manuf. Technol.*, 2007, **33**, 86–94.
13. Navarro, A., Rocks, S. A. and Dorey, R. A., Micromoulding of lead zirconate titanate (PZT) structures for MEMS. *J. Electroceram.*, 2007, **19**, 321–326.
14. Zhao, X., Evans, J. R. G. and Edirisinghe, M. J., Direct ink-jet printing of vertical walls. *J. Am. Ceram. Soc.*, 2002, **85**, 2113–2115.
15. Jaworek, A. and Krupa, A., Classification of the modes of EHD spraying. *J. Aerosol Sci.*, 1999, **30**, 873–893.
16. Jaworek, A., Electrospray droplet sources for thin film deposition. *J. Mater. Sci.*, 2007, **42**, 266–297.
17. Jaworek, A., Micro- and nanoparticle production by electrospraying. *Powder Technol.*, 2007, **176**, 18–35.
18. Jayasinghe, S. N. and Edirisinghe, M. J., A novel process for simultaneous printing of multiple tracks from concentrated suspensions. *Mater. Res. Innov.*, 2003, **7**, 62–64.
19. Wang, D. Z., Jayasinghe, S. N. and Edirisinghe, M. J., High resolution print-patterning of a nano-suspension. *J. Nanopart. Res.*, 2005, **7**, 301–306.
20. Sun, D., Rocks, S. A., Edirisinghe, M. J., Dorey, R. A. and Wang, Y., Electrohydrodynamic deposition of nanostructured lead zirconate titanate. *J. Nanosci. Nanotechno.*, 2005, **5**, 1846–1851.
21. Dorey, R. A., Dauchy, F., Wang, D. and Berriet, R., Fabrication and characterisation of annular thickness mode piezoelectric micro ultrasonic transducers. *IEEE T. Ultrason. Ferr.*, 2007, **54**, 2462–2468.
22. Dorey, R. A., Duval, F. F. C., Haigh, R. D. and Whatmore, R. W., The effect of repeated sol infiltrations on the microstructure and electrical properties of PZT composite sol–gel films. *Ferroelectrics*, 2002, **267**, 373–378.
23. Mani, B., Effect of heat and moisture on thick positive photoresist. In *Proceedings of the seventh IEEE/CHMT international electronic manufacturing technology symposium—integration of the manufacturing flow –from raw material through systems-level assembly*. IEEE, New York, 1989. pp. 310–313.
24. Kubenz, M., Ostrzinski, U., Reuther, F. and Gruetzner, G., Effective baking of thick and ultra-thick photoresist layers by infrared radiation. *Microelectron. Eng.*, 2003, **67–68**, 495–501.
25. Wang, Z. H., Miao, J. M. and Zhu, W. G., Piezoelectric thick films and their application in MEMS. *J. Eur. Ceram. Soc.*, 2007, **27**, 3759–3764.
26. Dorey, R. A., Whatmore, R. W., Beeby, S. P., Torah, R. N. and White, N. M., Screen printed PZT composite thick films. *Integr. Ferroelectr.*, 2004, **63**, 601–604.
27. Dorey, R. A., Stringfellow, S. B. and Whatmore, R. W., Effect of sintering aid and repeated sol infiltrations on the dielectric and piezoelectric properties of a PZT composite thick film. *J. Eur. Ceram. Soc.*, 2002, **22**, 2921–2926.